
STREAMING DATA RECOVERY VIA BAYESIAN TENSOR TRAIN DECOMPOSITION

Yunyu Huang, Yani Feng, Qifeng Liao*

School of Information Science and Technology
ShanghaiTech University
Shanghai, 201210, China

{edenhyy@foxmail.com, fengyn@shanghaitech.edu.cn, liaoqf@shanghaitech.edu.cn}

ABSTRACT

In this paper, we study a Bayesian tensor train (TT) decomposition method to recover streaming data by approximating the latent structure in high-order streaming data. Drawing on the streaming variational Bayes method, we introduce the TT format into Bayesian tensor decomposition methods for streaming data, and formulate posteriors of TT cores. Thanks to the Bayesian framework of the TT format, the proposed algorithm (SPTT) excels in recovering streaming data with high-order, incomplete, and noisy properties. The experiments in synthetic and real-world datasets show the accuracy of our method compared to state-of-the-art Bayesian tensor decomposition methods for streaming data.

Keywords Variational inference · Tensor train decomposition · Streaming tensor

1 Introduction

1.1 Motivation

In recent decades, there has been tremendous interest in streaming data recovery across diverse domains such as recommendation systems [1], sensor networks [2], and social media analytics [3]. Streaming data, characterized by its continuous generation and real-time flow, is susceptible to corruption during transmission and storage, leading to considerable difficulties in data analysis. Tensor decomposition is an important tool to represent and recover tensor data by introducing its latent structure. In practical applications, the latent structure is discovered by minimizing the reconstruction error of noisy observed tensor elements and then can be used to predict missing elements.

Effective numerical techniques, such as CANDECOMP/PARAFAC (CP) decomposition [4, 5, 6] Tucker decomposition [7, 8], and tensor train (TT) decomposition [9, 10], are frequently used for tensor decomposition and have been proposed to compress full tensors to obtain their latent representations, i.e., the latent structures. Although these techniques have achieved great success, they require processing on static data, meaning that the entire observed data is utilized at each iteration step. However, in practical scenarios such as log files from web application [11] and information from social networks [12], only partial observed elements are generated at each time step, and previously produced observed elements cannot be retrieved due to the stress on database capacity and privacy. Consequently, the techniques above will be unsuitable, prompting the necessity to update the latent structure online based on the current observed elements, and recover missing elements using the latent structure.

1.2 Related Work

Using CP decomposition to recover streaming data originated in [13], while subsequent enhancements are proposed by [14, 15, 16]. To analyze streaming data with multi-index structures commonly encountered in real scenarios, successive CP decomposition based algorithms like MAST [17], OR-MSTC [18], InParTen2 [19], and DisMASTD [20] have

*Corresponding author

emerged. In [21, 22], a dynamic tensor analysis (DTA) algorithm is proposed to approximate latent structure of Tucker decomposition. The Rapid Incremental Singular Value Decomposition (ISVD), introduced by [23, 24], streamlines the solution process within the DTA framework.

Meanwhile, Bayesian inference offers a promising approach for tackling the challenge of tensor decomposition in streaming data recovery. The forefront Bayesian tensor decomposition algorithms for streaming data include POST [25] and BASS-Tucker [26], grounded in the Bayesian formulations of CP and Tucker decomposition, respectively. While both POST and BASS-Tucker serve as robust streaming decomposition methods adaptable to various applications, two key challenges in modeling and computation for estimating the latent structure warrant attention. Firstly, the latent structures (CP and Tucker formats) in POST and BASS-Tucker struggle to effectively balance representation power and computational efficiency for high-order tensors. Secondly, in Bayesian tensor decomposition algorithms for streaming data, the design of a reliable prior for the latent structure is crucial for successful estimation.

1.3 Contributions

We introduce SPTT, a Streaming Probabilistic Tensor Train decomposition approach, for recovering streaming data by estimating the posterior of TT format. The contributions of our work are threefold:

- First, SPTT is founded on TT decomposition, combining the benefits of CP and Tucker decomposition. This stems from its provision of a space-saving model known as TT format while retaining strong representation capabilities.
- Second, inspired by the Bayesian TT representation for static data in [27], we devise a robust Gaussian prior of TT-cores tailored for streaming data. We employ the streaming variational Bayes (SVB) method on the Gaussian prior for streaming data analysis.
- Third, both synthetic and real-world data are used to demonstrate the accuracy of our algorithm.

2 Preliminaries

Throughout the paper, we denote scalar, vector, matrix and tensor variables, respectively, by lowercase letters (e.g. x), boldface lowercase letters (e.g. \mathbf{x}), boldface capital letters (e.g. \mathbf{X}), and boldface Euler script letters (e.g. \mathfrak{X}). For a D -th order tensor $\mathfrak{X} \in \mathbb{R}^{N_1 \times \dots \times N_D}$, the $\mathbf{j} := (j_1, \dots, j_D)$ -th element of \mathfrak{X} is defined by $x_{\mathbf{j}}$, where $j_d = 1, \dots, N_d$ for $d = 1, \dots, D$.

2.1 Tensor Train Decomposition

Tensor decomposition introduces a latent structure to represent the each element of tensors. We aim to infer the latent structure from incomplete noisy observed tensors. Tensor train (TT) decomposition has a great representation ability, especially for high-order tensors. Given a D -th order tensor \mathfrak{X} , the tensor train decomposition [9] is

$$x_{\mathbf{j}} \approx \prod_{d=1}^D \mathfrak{g}_{j_d}^{(d)}, \quad (1)$$

where $\mathfrak{g}_{j_d}^{(d)} \in \mathbb{R}^{r_{d-1} \times r_d}$ is the j_d -th slice of TT-cores $\mathfrak{g}^{(d)} \in \mathbb{R}^{r_{d-1} \times N_d \times r_d}$, for $j_d = 1, \dots, N_d$, $d = 1, \dots, D$, and the “boundary condition” is $r_0 = r_D = 1$. The vector $[r_0, r_1, r_2, \dots, r_D]$ is referred to as TT-ranks. The element-wise form (1) is considered to be in the TT-format shown in Figure 1. In other words, TT decomposition is to decompose a D -th order tensor \mathfrak{X} into a sequence of three-way factor tensors. For convenience, a more compact form is given by

$$\mathfrak{X} \approx \langle \langle \mathfrak{g}^{(1)}, \dots, \mathfrak{g}^{(D)} \rangle \rangle. \quad (2)$$

where $\langle \langle \cdot \rangle \rangle$ is a shorthand of multi-linear product (1) in TT decomposition. To infer the latent structure $\mathfrak{g} = \{\mathfrak{g}^{(d)}\}_{d=1}^D$ from noisy observed elements, one can minimize the following reconstruction error,

$$\mathcal{L}(\mathfrak{g}) = \sum_{\mathbf{j} \in \Omega} \|x_{\mathbf{j}} - \prod_{d=1}^D \mathfrak{g}_{j_d}^{(d)}\|^2, \quad (3)$$

where Ω represents the index set of the whole observed data. The alternating least squares algorithm [28] is commonly used to update each TT core alternatively, given all the other fixed.

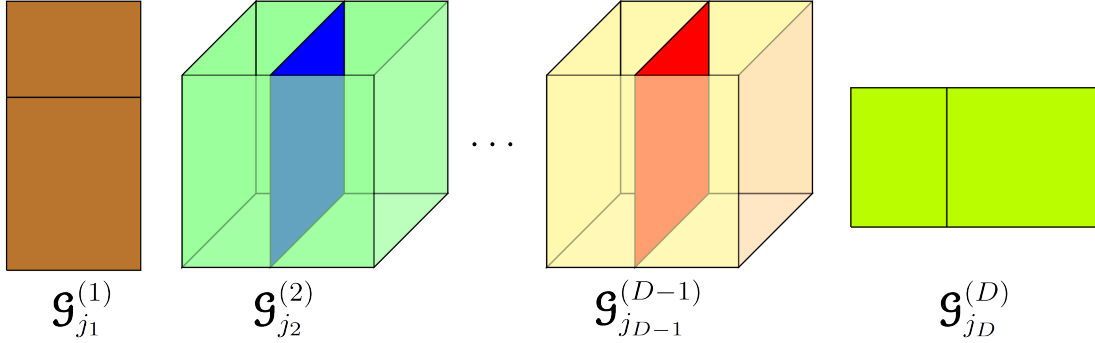


Figure 1: TT decomposition for an element x_j (TT-format).

2.2 Streaming Tensor Train Decomposition Problem Setting

The problem (3) need to conduct on static data, which implies that at each iteration step, one need to have access to the whole observed data. However, in practical application the observed data is generated dynamically. Due to the stress on database capacity and privacy, each time one only have access to the current observed data and cannot revisit the previously generated observed data. Moreover, traditional TT decomposition methods like [28, 29] use point estimation (3) to estimate TT-cores and is not capable of evaluating uncertainties, which can vary among each slice in TT-cores. To address the these issues, a new approach is developed for solving the streaming tensor decomposition problem and also estimating uncertainties.

Our goal is to infer TT-cores $\{\mathcal{G}^{(d)}\}_{d=1}^D$ from streaming data $\{B_1, B_2, \dots\} \subset B$, where $B_t = \{x_j | \mathbf{j} \in \Omega_t\}$ and Ω_t denotes its index set, but we can only visit data batch B_t at time t , instead of revisiting previous data $\tilde{B} = \{B_1, \dots, B_{t-1}\}$. The streaming variational Bayes (SVB) [30] method provides a Bayesian framework for the streaming TT decomposition problem, where uncertainties can be taken into consideration. Thus, we aim to find the posterior distribution of latent parameters θ including TT-cores from recursively received data. That is, to estimate the density function $p(\theta | \tilde{B}, B_t)$ with the current likelihood $p(B_t | \theta)$ and updated density function $p(\theta | \tilde{B})$ using the Bayes' rule as follows,

$$p(\theta | \tilde{B}, B_t) \propto p(\theta | \tilde{B}) p(B_t | \theta). \quad (4)$$

In Section 3.1, we will introduce a new probabilistic TT model, where the latent parameters is considered as random variables. Applying the SVB method, the recursively updating process (4) based on the probabilistic TT model can be achieved in Section 3.2.

3 Bayesian model for streaming tensor train decomposition

In this section, we first develop the probabilistic model of TT decomposition, where the Gaussian noise is included. After that, the posterior inference for TT-cores is conducted by the SVB method. Finally, we present the streaming probabilistic tensor train decomposition (SPTT) algorithm.

3.1 Probabilistic Modeling of Tensor Train Decomposition

Inspired by a Bayesian TT representation for static data in [27], we introduce a Bayesian TT model for streaming data. We first specify $\{\mathcal{G}^{(d)}\}_{d=1}^D$ from a Gaussian prior,

$$p(\{\mathcal{G}^{(d)}\}_{d=1}^D) = \prod_{d=1}^D \prod_{k=1}^{r_{d-1}} \prod_{l=1}^{r_d} \mathcal{N} \left(\mathcal{G}_{k::l}^{(d)} \middle| \mathbf{m}_{\mathcal{G}_{k::l}^{(d)}}, v \mathbf{I} \right), \quad (5)$$

which indicates that each fiber $\mathcal{G}_{k::l}^{(d)}$ admits a Gaussian distribution with mean $\mathbf{m}_{\mathcal{G}_{k::l}^{(d)}}$, and covariance matrix $v \mathbf{I}$. v is a scalar and controls the flatness of the Gaussian prior. In streaming TT decomposition problem, the prior in (5) is more reliable than the prior in [27], because the latter can fail to estimate TT-cores through a small amount of data by inducing TT-cores with all zeros elements.

Given TT-cores $\{\mathbf{g}^{(d)}\}_{d=1}^D$, the likelihood of an observed element x_j is

$$p(x_j|\{\mathbf{g}^{(d)}\}_{d=1}^D, \tau) = \mathcal{N}\left(x_j \mid \prod_{d=1}^D \mathbf{g}_{j_d}^{(d)}, \tau^{-1}\right), \quad (6)$$

where τ is the noise precision. Due to the non-negative and long tail, the Gamma distribution provides a good model for τ . We assign a Gamma prior over τ ,

$$p(\tau|\alpha_0, \beta_0) = \text{Gam}(\tau|\alpha_0, \beta_0), \quad (7)$$

where α_0 and β_0 are hyperparameters of the Gamma distribution. The joint probability is then given by combining (5) with (6)-(7),

$$\begin{aligned} p\left(x_{j \in \Omega}, \{\mathbf{g}^{(d)}\}_{d=1}^D, \tau\right) &= \text{Gam}(\tau|\alpha_0, \beta_0) \\ &\cdot \prod_{d=1}^D \prod_{k=1}^{r_{d-1}} \prod_{l=1}^{r_d} \mathcal{N}\left(\mathbf{g}_{k:,l}^{(d)} \mid \mathbf{m}_{\mathbf{g}_{k:,l}^{(d)}}, v\mathbf{I}\right) \\ &\cdot \prod_{j \in \Omega} \mathcal{N}\left(x_j \mid \prod_{d=1}^D \mathbf{g}_{j_d}^{(d)}, \tau^{-1}\right). \end{aligned} \quad (8)$$

3.2 Bayesian Streaming Inference

We propose a streaming probabilistic TT decomposition approach (SPTT) for streaming data, based on TT decomposition in section 3.1 and the streaming variational Bayes (SVB) [30]. For streaming data $\{B_1, B_2, \dots\}$ in Section 2.2, our goal is to conduct the posterior inference for each parameter in $\theta = \{\{\mathbf{g}^{(d)}\}_{d=1}^D, \tau\}$ upon receiving each data batch B_t , without revisiting the previous batches $\tilde{B} = \{B_1, \dots, B_{t-1}\}$.

The proportional relationship in (4) motivates us to conduct a recursive process of streaming inference for θ . However, the multilinear product of TT-cores $\{\mathbf{g}^{(d)}\}_{d=1}^D$ in (6) results in the posterior update intractable. To overcome the problem, we introduce a factorized variational posterior distribution $q^{(t-1)}(\theta) = \prod_i q_{\theta_i}^{(t-1)}(\theta_i)$ to approximate $p(\theta|\tilde{B})$ in the right hand-side of (4), where θ_i indicates a component in θ . With receiving new data batch B_t , we can obtain a new distribution

$$\tilde{p}^{(t)}(\theta) = q^{(t-1)}(\theta)p(B_t|\theta), \quad (9)$$

which is the product of posterior after $(t-1)$ -th data batch and the current likelihood of B_t and can be regarded as an approximation of the joint distribution $p(\theta, \tilde{B}, B_t)$ up to a normalization constant. More details for computing $\log \tilde{p}^{(t)}(\theta)$ can be found in Appendix C. Moreover, the current posterior $p(\theta|\tilde{B}, B_t)$ in left hand-side of (4) can be approximated by $q^{(t)}(\theta)$,

$$p(\theta|\tilde{B}, B_t) \approx q^{(t)}(\theta) = q_\tau^{(t)}(\tau) \prod_{d=1}^D \prod_{k=1}^{r_{d-1}} \prod_{l=1}^{r_d} \prod_{j_d}^{N_d} q_{\mathbf{g}_{k:,j_d,l}^{(d)}}^{(t)}\left(\mathbf{g}_{k:,j_d,l}^{(d)}\right). \quad (10)$$

based on the only assumption that each elements in TT-cores and the noise precision are independent. To be noticed, $q^{(t)}(\theta)$ is also in a factorized form as $q^{(t-1)}(\theta)$, and can be initialized with $q^{(0)}(\theta) = p(\theta)$, where $p(\theta)$ is the prior distribution θ and equals to the product of (5) and (7). From the variational inference framework [31], $q^{(t)}(\theta)$ is obtained by minimizing the Kullback-Leibler (KL) divergence between $\frac{1}{C}\tilde{p}^{(t)}(\theta)$ and $q^{(t)}(\theta)$, i.e. $\text{KL}(\frac{1}{C}\tilde{p}^{(t)}(\theta)||q^{(t)}(\theta))$, where C is a normalization constant. This is equivalent to maximize a variational model evidence lower bound (ELBO) [31],

$$\mathcal{L}(q^{(t)}(\theta)) = \mathbb{E}_{q^{(t)}} \left[\log \left(\frac{\tilde{p}^{(t)}(\theta)}{q^{(t)}(\theta)} \right) \right]. \quad (11)$$

Due to the factorized form (10), the closed form of the individual factors $q_{\theta_i}^{(t)}(\theta_i)$ can be explicitly derived. To be specific, $q_{\theta_i}^{(t)}(\theta_i)$ based on the maximization of $\mathcal{L}(q^{(t)}(\theta))$ is then given by

$$\log q_{\theta_i}^{(t)}(\theta_i) = \mathbb{E}_{q^{(t)}(\theta \setminus \theta_i)} \left[\log \tilde{p}^{(t)}(\theta) \right] + \text{const}, \quad (12)$$

where $\mathbb{E}_{q^{(t)}(\theta \setminus \theta_i)}$ denotes an expectation w.r.t the $q^{(t)}(\theta)$ distributions over all variables θ except θ_i .

3.2.1 Posterior Distribution of TT-cores

Upon the factorized form (10), the inference of an element of TT-cores $\mathbf{g}_{k,j_d,l}^{(d)}$ can be performed by receiving the messages from the t -th data batch B_t and the updated information of the whole TT-cores, where $k = 1, \dots, r_{d-1}$, $l = 1, \dots, r_d$, $j_d = 1, \dots, N_d$. By applying (12), the optimized form of $\mathbf{g}_{k,j_d,l}^{(d)}$ is given as follows,

$$\log q_{\mathbf{g}_{k,j_d,l}^{(d)}}^{(t)}(\mathbf{g}_{k,j_d,l}^{(d)}) = \mathbb{E}_{q^{(t)}(\theta \setminus \mathbf{g}_{k,j_d,l}^{(d)})} \left[\log \tilde{p}^{(t)}(\theta) \right] + \text{const}. \quad (13)$$

Obviously, the approximation posterior keeps the same form as the updated one, i.e., Gaussian distribution,

$$q_{\mathbf{g}_{k,j_d,l}^{(d)}}^{(t)}(\mathbf{g}_{k,j_d,l}^{(d)}) = \mathcal{N}(\mathbf{g}_{k,j_d,l}^{(d)} | \mu_{\mathbf{g}_{k,j_d,l}^{(d)}}^{(t)}, \nu_{\mathbf{g}_{k,j_d,l}^{(d)}}^{(t)}). \quad (14)$$

where (t) represents receiving the t -th data batch B_t . Here the variance and mean can be updated by

$$\nu_{\mathbf{g}_{k,j_d,l}^{(d)}}^{(t)} = \left(\nu_{\mathbf{g}_{k,j_d,l}^{(d)}}^{(t-1)}^{-1} + \mathbb{E}[\tau] \cdot \sum_{\mathbf{j} \in \Omega_t^{j_d}} \mathbb{E} \left[b_{(k-1)r_{d-1}+k}^{(<d)} \right] \mathbb{E} \left[b_{(l-1)r_d+l}^{(>d)} \right] \right)^{-1}, \quad (15)$$

$$\begin{aligned} \mu_{\mathbf{g}_{k,j_d,l}^{(d)}}^{(t)} &= \nu_{\mathbf{g}_{k,j_d,l}^{(d)}}^{(t)} \mu_{\mathbf{g}_{k,j_d,l}^{(d)}}^{(t-1)} \nu_{\mathbf{g}_{k,j_d,l}^{(d)}}^{(t-1)}^{-1} + \nu_{\mathbf{g}_{k,j_d,l}^{(d)}}^{(t)} \mathbb{E}[\tau] \sum_{\mathbf{j} \in \Omega_t^{j_d}} \left(x_{\mathbf{j}} \mathbb{E} \left[e_k^{(<d)} \right] \mathbb{E} \left[e_l^{(>d)} \right] \right. \\ &\quad \left. - \sum_{k'=1}^{r_{d-1}} \sum_{l'=1}^{r_d} \mathbb{E} \left[b_{(k-1)r_{d-1}+k'}^{(<d)} \right] \mathbb{E} \left[b_{(l-1)r_d+l'}^{(>d)} \right] \mu_{\mathbf{g}_{k',j_d,l'}}^{(t-1)} + \mathbb{E} \left[b_{(k-1)r_{d-1}+k}^{(<d)} \right] \mathbb{E} \left[b_{(l-1)r_d+l}^{(>d)} \right] \mu_{\mathbf{g}_{k,j_d,l}^{(d)}}^{(t-1)} \right), \end{aligned} \quad (16)$$

with

$$\mathbb{E} \left[e^{(<d)} \right] = \prod_{i=1}^{d-1} \mathbb{E} \left[\mathbf{g}_{j_i}^{(i)} \right], \quad \mathbb{E} \left[e^{(>d)} \right] = \prod_{i=d+1}^D \mathbb{E} \left[\mathbf{g}_{j_i}^{(i)} \right], \quad (17)$$

$$\begin{aligned} \mathbb{E} \left[b^{(<d)} \right] &= \prod_{i=1}^{d-1} \mathbb{E} \left[\mathbf{g}_{j_i}^{(i)} \otimes \mathbf{g}_{j_i}^{(i)} \right], \\ \mathbb{E} \left[b^{(>d)} \right] &= \prod_{i=d+1}^D \mathbb{E} \left[\mathbf{g}_{j_i}^{(i)} \otimes \mathbf{g}_{j_i}^{(i)} \right], \end{aligned} \quad (18)$$

where $\nu_{\mathbf{g}_{k,j_d,l}^{(d)}}^{(t)}$ and $\mu_{\mathbf{g}_{k,j_d,l}^{(d)}}^{(t)}$ are the variance and mean of the element $\mathbf{g}_{k,j_d,l}^{(d)}$ at the t -th data batch. The subscript $\Omega_t^{j_d}$ represents the indexes of t -th batch data with d -th index fixing as j_d . The expression $\mathbb{E}[\cdot]$ denotes the expectation with respect to all random variables involved. From (17) and (18), we can see that, for $d = 1, \dots, D$, $e^{(<d)}$ and $b^{(<d)}$ are row vectors, while $e^{(>d)}$ and $b^{(>d)}$ are column vectors. The subscript of them denotes an element of a vector, e.g. $e_k^{(<d)}$ is the k -th element of vector $e^{(<d)}$. The derivations of (15) and (16) are illustrated in Appendix A.

The variance and mean of TT-cores can be initialized by (5), i.e., $q_{\mathbf{g}}^{(0)}(\mathbf{g}) = p(\mathbf{g})$. Moreover, we introduce the following proposition from [27] to compute $\mathbb{E} \left[\mathbf{g}_{j_i}^{(i)} \otimes \mathbf{g}_{j_i}^{(i)} \right]$ in (18).

Proposition 3.1. *The expectation of Kronecker product $\mathbf{g}_{j_i}^{(i)} \otimes \mathbf{g}_{j_i}^{(i)}$ in (18) can be calculated by*

$$\mathbb{E} \left[\mathbf{g}_{j_i}^{(i)} \otimes \mathbf{g}_{j_i}^{(i)} \right] = \mathbb{E} \left[\mathbf{g}_{j_i}^{(i)} \right] \otimes \mathbb{E} \left[\mathbf{g}_{j_i}^{(i)} \right] + \mathbb{E} \left[\left(\mathbf{g}_{j_i}^{(i)} - \mathbb{E} \left[\mathbf{g}_{j_i}^{(i)} \right] \right) \otimes \left(\mathbf{g}_{j_i}^{(i)} - \mathbb{E} \left[\mathbf{g}_{j_i}^{(i)} \right] \right) \right],$$

Proof. From equation (10), we can see any two elements in $\mathbf{g}_{j_i}^{(i)}$ are independent,

$$\mathbb{E} \left[\mathbf{g}_{k,j_i,l}^{(i)} \mathbf{g}_{k',j_i,l'}^{(i)} \right] = \mathbb{E} \left[\mathbf{g}_{k,j_i,l}^{(i)} \right] \mathbb{E} \left[\mathbf{g}_{k',j_i,l'}^{(i)} \right] + v_{\mathbf{g}_{k,j_i,l}^{(i)}} \delta(k-k') \delta(l-l').$$

where $\delta(x) = 1$ if $x = 0$ and zero otherwise. Let $p = r_{i-1}(k-1) + k'$, $q = r_i(l-1) + l'$, then

$$\mathbb{E} \left[\mathbf{g}_{j_i}^{(i)} \otimes \mathbf{g}_{j_i}^{(i)} \right]_{p,q} = \left(\mathbb{E} \left[\mathbf{g}_{j_i}^{(i)} \right] \otimes \mathbb{E} \left[\mathbf{g}_{j_i}^{(i)} \right] \right)_{p,q} + \mathbf{v}_{p,j_i,q}^{(i)}$$

where

$$\mathbf{v}_{j_d}^{(i)} := \mathbb{E} \left[\left(\mathbf{g}_{j_d}^{(i)} - \mathbb{E} \left[\mathbf{g}_{j_d}^{(i)} \right] \right) \otimes \left(\mathbf{g}_{j_d}^{(i)} - \mathbb{E} \left[\mathbf{g}_{j_d}^{(i)} \right] \right) \right]. \quad (19)$$

As a Kronecker-form covariance, $\mathbf{V}_{j_d}^{(i)} \in \mathbb{R}^{r_{i-1}^2 \times r_i^2}$ consists of block matrices with dimension $r_{i-1} \times r_i$ and the (k, l) -th block matrix contains only one nonzero element $v_{\mathbf{g}_{k,j_i,l}^{(i)}}$ at the (k, l) -th position. Thus,

$$\mathbb{E} \left[\mathbf{g}_{j_d}^{(i)} \otimes \mathbf{g}_{j_d}^{(i)} \right] = \mathbb{E} \left[\mathbf{g}_{j_d}^{(i)} \right] \otimes \mathbb{E} \left[\mathbf{g}_{j_d}^{(i)} \right] + \mathbf{v}_{j_d}^{(i)}.$$

□

3.2.2 Posterior Distribution of Noise Precision

Following equation (12), the update for the noise precision τ can be derived by rearranging the equation as follows,

$$\log q_\tau^{(t)}(\tau) = \mathbb{E}_{q^{(t)}(\theta \setminus \tau)} \left[\log \tilde{p}^{(t)}(\theta) \right] + \text{const}, \quad (20)$$

from which, we can see the posterior of noise precision τ is also a Gamma distribution,

$$q_\tau^{(t)}(\tau) = \text{Gam}(\tau | \alpha^{(t)}, \beta^{(t)}), \quad (21)$$

and the posterior hyperparameters can be updated by

$$\alpha^{(t)} = \alpha^{(t-1)} + \frac{|\Omega_t|}{2}, \quad (22)$$

$$\beta^{(t)} = \beta^{(t-1)} + \frac{1}{2} \mathbb{E} \left[\sum_{\mathbf{j} \in \Omega_t} \left(x_{\mathbf{j}} - \prod_{d=1}^D \mathbf{g}_{j_d}^{(d)} \right)^2 \right], \quad (23)$$

where

$$\mathbb{E} \left[\sum_{\mathbf{j} \in \Omega_t} \left(x_{\mathbf{j}} - \prod_{d=1}^D \mathbf{g}_{j_d}^{(d)} \right)^2 \right] = \mathbf{x}_{\Omega_t}^T (\mathbf{x}_{\Omega_t} - 2\mathbf{A}_{\Omega_t}) + \sum_{\mathbf{j} \in \Omega_t} \prod_{d=1}^D \left(\mathbb{E} \left[\mathbf{g}_{j_d}^{(d)} \right] \otimes \mathbb{E} \left[\mathbf{g}_{j_d}^{(d)} \right] + \mathbf{v}_{j_d}^{(d)} \right). \quad (24)$$

Appendix B provides more details about the update formula. From (22), we can see that the shape parameter updates with the number of the newly receiving data batch B_t . The summation term in (23) controls the noise precision τ through the rate parameter $\hat{\beta}$. It is seen in (23) that when the model dose not fit the streaming data well, there is an increase in $\hat{\beta}$ and thus a decrease in the noise variance since $\mathbb{E}[\tau] = \hat{\alpha}/\hat{\beta}$. Computing (24) is challenging, so we present a proposition as follows.

Proposition 3.2. *Given a set of independent random matrices $\{\mathbf{g}_{j_d}^{(d)}\}_{d=1}^D$, we assume that $\forall d \in \{1, \dots, D\}, \forall k \in \{1, \dots, r_{d-1}\}, \forall l \in \{1, \dots, r_d\}$, the vectors $\{\mathbf{g}_{k, :, l}^{(d)}\}$ are independent, then*

$$\mathbb{E} \left[\left(\prod_{d=1}^D \mathbf{g}_{j_d}^{(d)} \right)^2 \right] = \prod_{d=1}^D \left(\mathbb{E} \left[\mathbf{g}_{j_d}^{(d)} \right] \otimes \mathbb{E} \left[\mathbf{g}_{j_d}^{(d)} \right] + \mathbf{v}_{j_d}^{(d)} \right).$$

Proof. For a scalar $\prod_{d=1}^D \mathbf{g}_{j_d}^{(d)}$, using the mix product property of Kronecker product and conclusion of proposition 3.1, we have

$$\begin{aligned} \mathbb{E} \left[\left(\prod_{d=1}^D \mathbf{g}_{j_d}^{(d)} \right)^2 \right] &= \mathbb{E} \left[\left(\prod_{d=1}^D \mathbf{g}_{j_d}^{(d)} \right) \otimes \left(\prod_{d=1}^D \mathbf{g}_{j_d}^{(d)} \right) \right] \\ &= \prod_{d=1}^D \mathbb{E} \left[\left(\mathbf{g}_{j_d}^{(d)} \otimes \mathbf{g}_{j_d}^{(d)} \right) \right] \\ &= \prod_{d=1}^D \left(\mathbb{E} \left[\mathbf{g}_{j_d}^{(d)} \right] \otimes \mathbb{E} \left[\mathbf{g}_{j_d}^{(d)} \right] + \mathbf{v}_{j_d}^{(d)} \right), \end{aligned}$$

where $\mathbf{v}_{j_d}^{(d)}$ is defined in (19). □

3.2.3 Algorithm

Since the ELBO in (11) is only guaranteed to converge to a local maximum[32], a good initialization is important. The noise precision τ in (7) is initialized as $q_\tau^{(0)}(\tau) = \text{Gam}(\tau|\alpha_0, \beta_0)$ where $\alpha_0 = \beta_0 = 10^{-3}$, and then $\mathbb{E}_{q_\tau^{(0)}}[\tau] = 1$. For TT-cores $\{\mathbf{g}^{(d)}\}_{d=1}^D$ in (5), each fiber $\mathbf{g}_{k,:,l}^{(d)}$ is initialized as,

$$q_{\mathbf{g}_{k,:,l}^{(d)}}^{(0)}(\mathbf{g}_{k,:,l}^{(d)}) = \mathcal{N}(\mathbf{g}_{k,:,l}^{(d)} | \mathbf{m}_{\mathbf{g}_{k,:,l}^{(d)}}, \mathbf{I}), \quad (25)$$

where each element of $\mathbf{m}_{\mathbf{g}_{k,:,l}^{(d)}}$ is generated from a standard uniform distribution $U(0, 1)$. Then $\mathbb{E}_{q_{\mathbf{g}^{(d)}}^{(0)}}(\mathbf{g}^{(d)}) = \mathbf{m}_{\mathbf{g}^{(d)}}$, where $\mathbf{m}_{\mathbf{g}^{(d)}}$ is a tensor with the same size as $\mathbf{g}^{(d)}$ and collects the fibers $\mathbf{g}_{k,:,l}^{(d)}$, for $k = 1, \dots, r_d, l = 1, \dots, r_{d-1}$.

Our SPTT algorithm is summarized in Algorithm 1, where we stop the algorithm and output the updated mean and variance of each TT-cores if the final data batch $B_{t_{\max}}$ is used.

Algorithm 1 Streaming probabilistic tensor train decomposition (SPTT)

Require: Data streams $\{B_1, \dots, B_{t_{\max}}\}$.

- 1: Initialize $q_\tau^{(0)}(\tau)$ using (7), $\alpha_0 = \beta_0 = 10^{-3}$, then $\mathbb{E}_{q_\tau^{(0)}}[\tau] = 1$.
- 2: Initialize $q_{\mathbf{g}^{(d)}}^{(0)}(\mathbf{g}^{(d)})$ using (25), for $d = 1, \dots, D$.
- 3: Set $t = 1$ and $\epsilon_{\mathcal{G}} = 1$.
- 4: **while** $t < t_{\max}$ **do**
- 5: Load the data batch B_t .
- 6: **while** Not converge **do**
- 7: **for** $d = 1$ to D **do**
- 8: Calculate $\mathbb{E}[e^{(<d)}], \mathbb{E}[b^{(<d)}], \mathbb{E}[e^{(>d)}], \mathbb{E}[b^{(>d)}]$ by (17) and (18).
- 9: Update $q_{\mathbf{g}^{(d)}}^{(t)}$ associated with B_t via (15) and (16).
- 10: Update $q_\tau^{(t)}$ via (22) and (23).
- 11: **end for**
- 12: **end while**
- 13: Let $t = t + 1$.
- 14: **end while**
- 15: Let $q_{\mathbf{g}^{(d)}}^* = q_{\mathbf{g}^{(d)}}^{(t_{\max})}$, $d = 1, \dots, D$.

Ensure: The updated posterior of TT-cores $q_{\mathbf{g}^{(d)}}^*$, $d = 1, \dots, D$.

The complexity of the proposed algorithm arises from updating the posterior of $\{\mathbf{g}^{(d)}\}_{d=1}^D$ and τ . For simplicity, we assume that all TT-ranks are initially set as L , the length in each order is N , and the batch size is S . In each streaming batch, updating of each TT core $\mathbf{g}^{(d)}$ involves $\mathcal{O}(DL^2)$ operations to get $e^{(<d)}$ and $e^{(>d)}$, $\mathcal{O}(DL^4)$ operations to obtain $b^{(<d)}$ and $b^{(>d)}$, $\mathcal{O}(SDL^2)$ operations to compute the mean and $\mathcal{O}(SDL^4)$ operations to calculate the variance of a TT core in (15) and (16) respectively. Furthermore, computing each τ requires $\mathcal{O}(SD(L^4 + L^2))$ operations. Thus, the overall time complexity is $\mathcal{O}(SDL^4)$. Thus, the overall time complexity is $\mathcal{O}(SDL^4)$. The space complexity is $\mathcal{O}(NDL^2)$, which is required to store the posterior mean and variance of $\{\mathbf{g}^{(d)}\}_{d=1}^D$.

4 Experiments

Based on both high-order synthetic and real-world applications, our SPTT are compared with related decomposition methods, including Bayesian streaming tensor decomposition methods: POST [25], BASS-Tucker [26], and static tensor decomposition methods: CP-ALS [33], CP-WOPT [34], Tucker-ALS [35]. All results of this paper are obtained in MATLAB (2022a) on a computer with an Intel(R) Core(TM) i7-8650U CPU @ 1.90GHz 2.11 GHz.

4.1 Synthetic Data

The synthetic tensor data is generated by the following procedure. Through TT decomposition in (1), we create a true tensor $\mathcal{A} \in \mathbb{R}^{20 \times 20 \times 20 \times 20}$ in TT-format with the TT-ranks $(1, 3, 3, 3, 1)$ by sampling the elements of TT-cores $\{\mathbf{g}^{(d)}\}_{d=1}^4$ from standard uniform distribution $U(0, 1)$, and $\mathcal{A} = \langle\langle \mathbf{g}^{(1)}, \mathbf{g}^{(2)}, \mathbf{g}^{(3)}, \mathbf{g}^{(4)} \rangle\rangle$. The synthetic observed

tensor \mathcal{U} is generated as follows,

$$\mathcal{U} = \mathcal{A} + \mathcal{W}, \quad (26)$$

where \mathcal{W} is a Gaussian noise tensor with its element $w_j \sim \mathcal{N}(0, \sigma^2)$ and σ is noise level, controlled by signal-to-noise-ratio (SNR),

$$\text{SNR} = 10 \log \left(\frac{\text{var}(\mathcal{A})}{\sigma^2} \right). \quad (27)$$

In order to investigate the ability of our streaming decomposition algorithm, the ratio of the number of observed tensor elements to the total tensor elements is set to 15%, and the indexes of observed elements are chosen randomly. We divide 10% observed elements into the test set T , remaining 90% of observed elements into the training set B . Then the training set B is randomly partitioned into a stream of small data batches $\{B_1, B_2, \dots, B_{t_{\max}}\}$. The batch size is denoted by S , then $t_{\max} = |B|/S$ in Algorithm 1, where $|B|$ is the total number of the training set. Moreover, the entire observed data is input to the static decomposition algorithms (CP-ALS, CP-WOPT, and Tuckers-ALS). The maximum iteration number is set to $M = 100$ in Algorithm 1, and TT-ranks of initial TT-cores are denoted by a vector $(1, R, R, R, 1)$. In related tensor decomposition methods experiments, default settings are used for maximum iteration number and initialization.

Denote $\hat{\mathcal{A}}$ as the TT-format tensor formulated by the updated posterior mean of TT-cores. To evaluate the performance of the above tensor decomposition approaches, the following relative error ϵ is used as reconstruction criterion,

$$\epsilon = \frac{\|\hat{\mathcal{A}}_T - \mathcal{A}_T\|_F}{\|\mathcal{A}_T\|_F}. \quad (28)$$

where $\hat{\mathcal{A}}_T$ denote a vector contains elements of tensor $\hat{\mathcal{A}}$ on test set T .

Next, our SPTT is compared with related tensor decomposition methods (POST, BASS-Tucker, CP-ALS, CP-WOPT and Tucker-ALS) regarding the relative reconstruction error under different batch sizes S , different initial rank R , and different SNR. To be noticed, the rank R in CP, Tucker and TT decomposition denotes the CP-rank R , Tucker-ranks (R, R, R, R) and TT-ranks $(1, R, R, R, 1)$ respectively. All tensor decomposition algorithms are repeated 5 times, and the calculated average relative error and standard deviation are shown in Fig. 2. In Fig. 2 (a), the settings are the fixed rank $R = 3$, $\text{SNR} = 20$, and different choices of batch sizes $S \in \{2^8, 2^9, 2^{10}, 2^{11}\}$. In Fig. 2 (b), the settings are the fixed streaming batch size $S = 512$, $\text{SNR} = 20$, and different rank $R \in \{3, 4, 5, 6\}$. In Fig. 2 (c), the settings are $S = 512$, $R = 3$, and different noise level $\text{SNR} \in \{15, 20, 25, 30\}$. As we can see, SPTT outperforms BASS-Tucker, POST and static decomposition methods in all the cases.

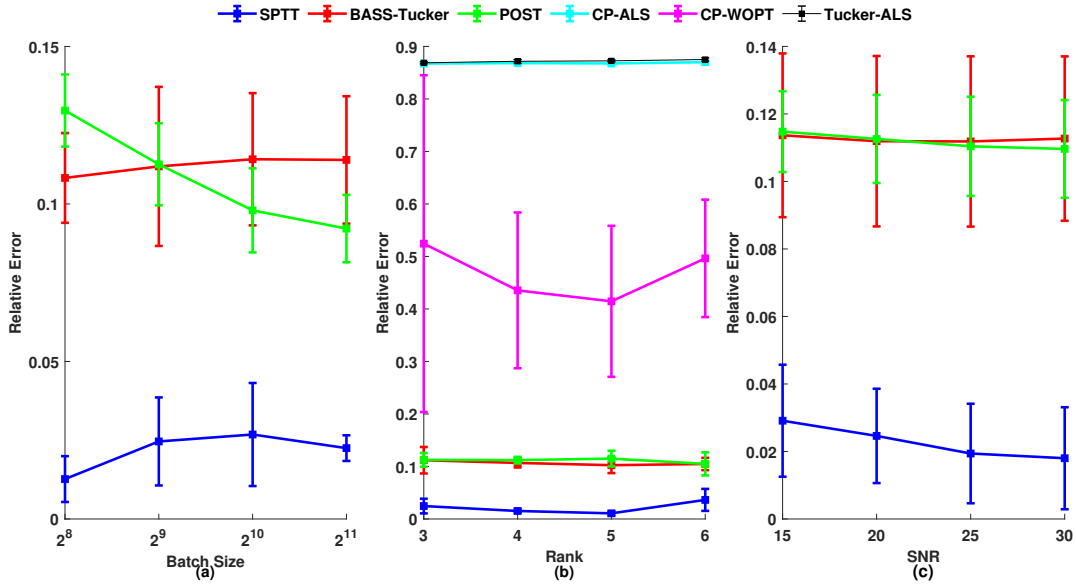


Figure 2: Predictive performance of synthetic data under different conditions.

In addition, the running predictive performance of SPTT is evaluated. We fix the batch size $S = 512$, $\text{SNR} = 20$, and gradually feed the training set $\{B_1, B_2, \dots, B_{t_{\max}}\}$ to SPTT, BASS-Tucker and POST. Two cases ($R = 3, 5$) are

considered to test the prediction accuracy after each data batch is used. The corresponding running relative error is shown in Fig. 3. As we can see, the relative error of our SPTT is clearly smaller than that of POST and BASS-Tucker, which demonstrates the accuracy of our SPTT.

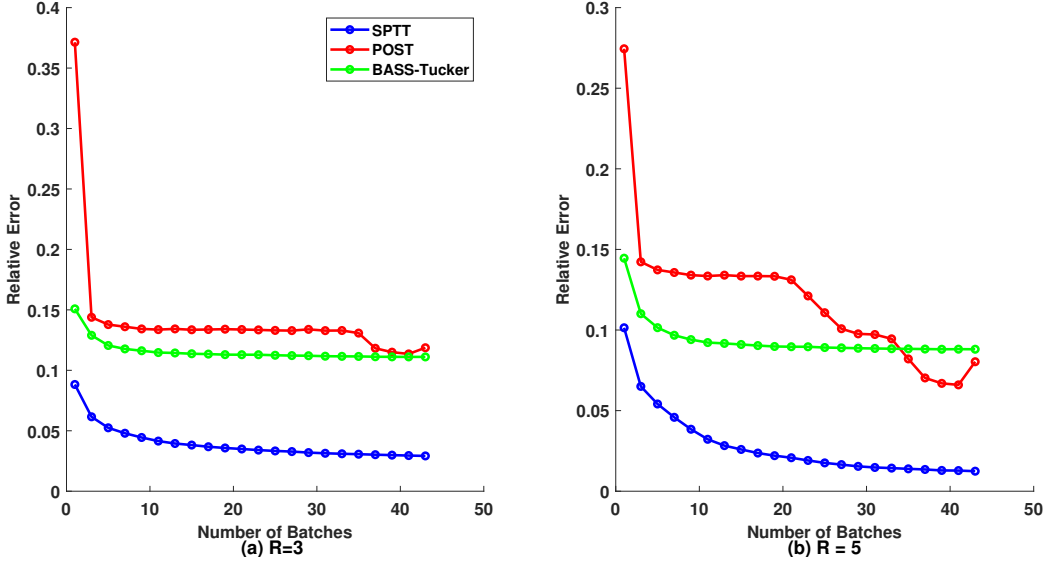


Figure 3: The running predictive performance of synthetic data.

4.2 Real-world Applications

To evaluate our SPTT, three cases of datasets (ALOG [36], Carphone [37], Flow injection²) are considered. ALOG data come from a three-mode (user, action, resource) tensor of size $200 \times 100 \times 200$ including 0.66% observed elements, which represents three-way management operations; Carphone data are extracted from a three-mode (length, width, frames) of video data of size $144 \times 176 \times 180$, which contains 0.5% nonzeros elements; Flow injection data, as a three-mode (samples, wavelengths, times) tensor of size $12 \times 100 \times 89$, are extracted from a flow injection analysis system and include 21360 nonzero elements.

Here our SPTT is compared with the related methods (POST, BASS-Tucker, CP-ALS, CP-WOPT, and Tucker-ALS) in terms of the relative reconstruction error ϵ defined in (28) under different batch size S and different initial rank R . To be noticed, the rank R in CP, Tucker and TT decomposition denotes the CP-rank R , Tucker-ranks (R, R, R) and TT-ranks $(1, R, R, 1)$ respectively. The maximum iteration number is set to $M = 100$ in Algorithm 1 and TT-ranks of initial TT-cores are set to $(1, R, R, 1)$. For maximum iteration number and initialization of all the related tensor decomposition methods, we use their corresponding default settings. The observed elements of Alog are randomly divided into 75% for training and 25% for testing, and for the other two datasets, their 10% observed elements are prepared for testing. For POST, SPTT, and BASS-Tucker, the training elements are randomly partitioned into a stream of small batches according to batch size S . Moreover, we input the whole observed data for static decomposition algorithms (CP-ALS, CP-WOPT, and Tucker-ALS). Fig. 4 reports the average relative error and standard deviation. In Fig. 4 (a)-(c), we fix the batch size $S = 512$ and show how the predictive performance of each method varies with different rank $R \in \{3, 4, 5, 6\}$. The bigger the rank, the more expensive for SPTT to factorize each batch. It can be seen from Fig. 4 (c), as the initial rank R increases from 3 to 5, the relative error of SPTT gradually increases and finally gets close to the relative error of POST. To test the capacity of decomposition algorithms on different batch sizes, we fix the rank $R = 3$, and test the performance with different choices of batch sizes $S \in \{2^8, 2^9, 2^{10}, 2^{11}\}$ in Fig. 4 (d)-(f). As we can see, SPTT outperforms BASS-Tucker, POST, and static decomposition methods for three datasets, especially for Carphone data.

The running predictive performance of SPTT is evaluated. We fix the batch size $S = 512$, and continuously feed the training set to SPTT, BASS-Tucker and POST. For the three datasets, two cases are considered, i.e. $R = 3$ and $R = 5$

²Retrieved from www.models.kvl.dk

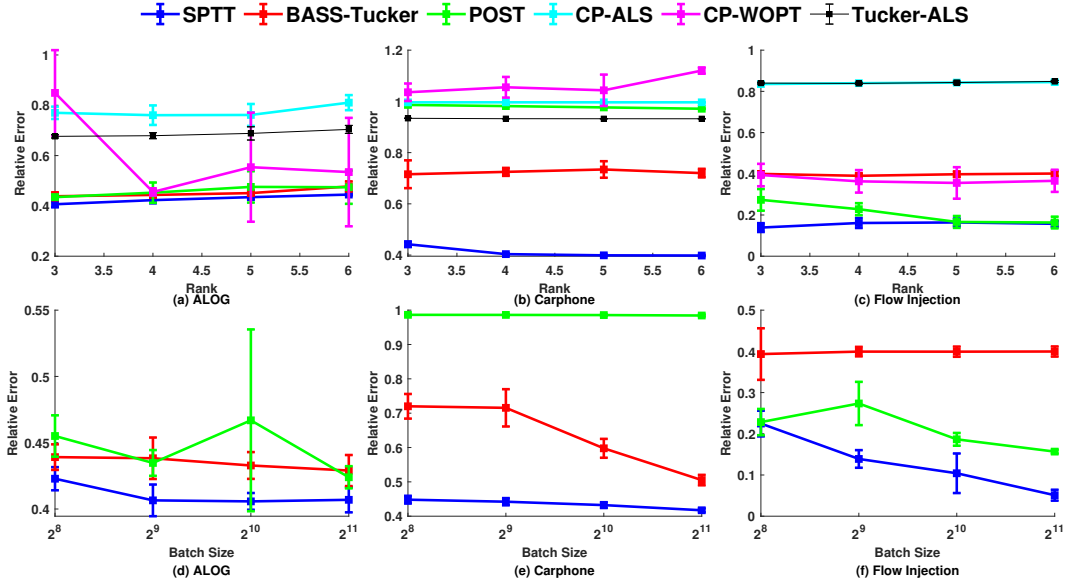


Figure 4: Predictive performance with different rank(top row) and streaming batch size (bottom row).

to test the prediction accuracy after each data batch is used. The running relative error is shown in Fig. 3. In all the cases, when the number of batches is small, POST or BASS-Tucker may performs better than SPTT. However, as the data streams, SPTT beats POST and BASS-Tucker gradually.

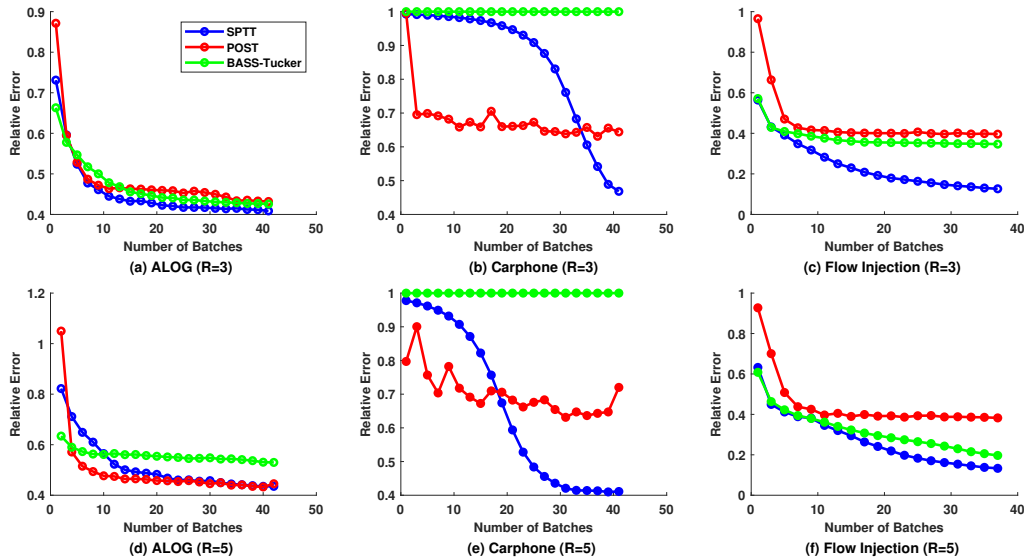


Figure 5: The running predictive performance in real-world applications.

5 CONCLUSIONS

In this paper, we propose a novel Bayesian streaming tensor decomposition algorithm, namely SPTT, to find the latent structure approximation from high-order incomplete and noisy streaming data and predict missing values. Leveraging

TT decomposition and a customized Gaussian prior, SPTT addresses key challenges in high-order streaming data recovery. Numerical experiments show that our SPTT algorithm can produce accurate predictions on synthetic and real-world streaming data. For future work, we are interested in develop a sparse strategy based on SPTT to further prevent overfitting and enhance scalability.

References

- [1] Yanxiang Huang, Bin Cui, Wenyu Zhang, Jie Jiang, and Ying Xu. Tencentrec: Real-time stream recommendation in practice. In *Proceedings of the 2015 ACM SIGMOD international conference on management of data*, pages 227–238, 2015.
- [2] Yue Hu, Ao Qu, Yanbing Wang, and Daniel B Work. Streaming data preprocessing via online tensor recovery for large environmental sensor networks. *ACM Transactions on Knowledge Discovery from Data (TKDD)*, 16(6):1–24, 2022.
- [3] Joseph R Zipkin, Frederic P Schoenberg, Kathryn Coronges, and Andrea L Bertozzi. Point-process models of social network interactions: Parameter estimation and missing data recovery. *European journal of applied mathematics*, 27(3):502–529, 2016.
- [4] Richard A Harshman et al. Foundations of the parafac procedure: Models and conditions for an " explanatory" multimodal factor analysis. 1970.
- [5] Rasmus Bro. Parafac. tutorial and applications. *Chemometrics and intelligent laboratory systems*, 38(2):149–171, 1997.
- [6] Kejun Tang and Qifeng Liao. Rank adaptive tensor recovery based model reduction for partial differential equations with high-dimensional random inputs. *Journal of Computational Physics*, 409:109326, 2020.
- [7] Ledyard R Tucker. Some mathematical notes on three-mode factor analysis. *Psychometrika*, 31(3):279–311, 1966.
- [8] Chuanfu Xiao, Chao Yang, and Min Li. Efficient alternating least squares algorithms for low multilinear rank approximation of tensors. *Journal of Scientific Computing*, 87:1–25, 2021.
- [9] Ivan V Oseledets. Tensor-train decomposition. *SIAM Journal on Scientific Computing*, 33(5):2295–2317, 2011.
- [10] Yani Feng, Kejun Tang, Lianxing He, Pingqiang Zhou, and Qifeng Liao. Tensor train random projection. *arXiv preprint arXiv:2010.10797*, 2020.
- [11] Rita Roy and G Appa Rao. Survey on pre-processing web log files in web usage mining. *International Journal of Advanced Science and Technology*, 29(3 Special Issue):682–691, 2020.
- [12] Danai Koutra, Evangelos E Papalexakis, and Christos Faloutsos. Tensorsplat: Spotting latent anomalies in time. In *2012 16th Panhellenic Conference on Informatics*, pages 144–149. IEEE, 2012.
- [13] Dimitri Nion and Nicholas D Sidiropoulos. Adaptive algorithms to track the parafac decomposition of a third-order tensor. *IEEE Transactions on Signal Processing*, 57(6):2299–2310, 2009.
- [14] Truong Minh-Chinh, Viet-Dung Nguyen, Nguyen Linh-Trung, and Karim Abed-Meraim. Adaptive parafac decomposition for third-order tensor completion. In *2016 IEEE Sixth International Conference on Communications and Electronics (ICCE)*, pages 297–301. IEEE, 2016.
- [15] Viet-Dung Nguyen, Karim Abed-Meraim, and Nguyen Linh-Trung. Fast adaptive parafac decomposition algorithm with linear complexity. In *2016 IEEE International Conference on Acoustics, Speech and Signal Processing (ICASSP)*, pages 6235–6239. IEEE, 2016.
- [16] Viet-Dung Nguyen, Karim Abed-Meraim, and Nguyen Linh-Trung. Second-order optimization based adaptive parafac decomposition of three-way tensors. *Digital Signal Processing*, 63:100–111, 2017.
- [17] Qingquan Song, Xiao Huang, Hancheng Ge, James Caverlee, and Xia Hu. Multi-aspect streaming tensor completion. In *Proceedings of the 23rd ACM SIGKDD international conference on knowledge discovery and data mining*, pages 435–443, 2017.
- [18] Mehrnaz Najafi, Lifang He, and S Yu Philip. Outlier-robust multi-aspect streaming tensor completion and factorization. In *IJCAI*, pages 3187–3194, 2019.
- [19] Hye-Kyung Yang and Hwan-Seung Yong. Multi-aspect incremental tensor decomposition based on distributed in-memory big data systems. *Journal of Data and Information Science*, 5(2):13–32, 2020.
- [20] Keyu Yang, Yunjun Gao, Yifeng Shen, Baihua Zheng, and Lu Chen. Dismastd: An efficient distributed multi-aspect streaming tensor decomposition. In *Proceedings of the ACM Turing Award Celebration Conference-China 2023*, pages 127–128, 2023.

- [21] Jimeng Sun, Dacheng Tao, and Christos Faloutsos. Beyond streams and graphs: dynamic tensor analysis. In *Proceedings of the 12th ACM SIGKDD international conference on Knowledge discovery and data mining*, pages 374–383, 2006.
- [22] Jimeng Sun, Dacheng Tao, Spiros Papadimitriou, Philip S Yu, and Christos Faloutsos. Incremental tensor analysis: Theory and applications. *ACM Transactions on Knowledge Discovery from Data (TKDD)*, 2(3):1–37, 2008.
- [23] Xi Li, Weiming Hu, Zhongfei Zhang, Xiaoqin Zhang, and Guan Luo. Robust visual tracking based on incremental tensor subspace learning. In *2007 IEEE 11th international conference on computer vision*, pages 1–8. IEEE, 2007.
- [24] Weiming Hu, Xi Li, Xiaoqin Zhang, Xinchu Shi, Stephen Maybank, and Zhongfei Zhang. Incremental tensor subspace learning and its applications to foreground segmentation and tracking. *International Journal of Computer Vision*, 91:303–327, 2011.
- [25] Yishuai Du, Yimin Zheng, Kuang-chih Lee, and Shandian Zhe. Probabilistic streaming tensor decomposition. In *2018 IEEE International Conference on Data Mining (ICDM)*, pages 99–108. IEEE, 2018.
- [26] Shikai Fang, Robert M. Kirby, and Shandian Zhe. Bayesian streaming sparse tucker decomposition. In Cassio de Campos and Marloes H. Maathuis, editors, *Proceedings of the Thirty-Seventh Conference on Uncertainty in Artificial Intelligence*, volume 161 of *Proceedings of Machine Learning Research*, pages 558–567. PMLR, 27–30 Jul 2021.
- [27] Le Xu, Lei Cheng, Ngai Wong, and Yik-Chung Wu. Probabilistic tensor train decomposition with automatic rank determination from noisy data. In *2021 IEEE Statistical Signal Processing Workshop (SSP)*, pages 461–465, 2021.
- [28] Wenqi Wang, Vaneet Aggarwal, and Shuchin Aeron. Tensor completion by alternating minimization under the tensor train (tt) model. *arXiv preprint arXiv:1609.05587*, 2016.
- [29] Longhao Yuan, Qibin Zhao, Lihua Gui, and Jianting Cao. High-order tensor completion via gradient-based optimization under tensor train format. *Signal Processing: Image Communication*, 73:53–61, 2019. Tensor Image Processing.
- [30] Tamara Broderick, Nicholas Boyd, Andre Wibisono, Ashia C Wilson, and Michael I Jordan. Streaming variational bayes. *Advances in neural information processing systems*, 26, 2013.
- [31] Martin J Wainwright, Michael I Jordan, et al. Graphical models, exponential families, and variational inference. *Foundations and Trends® in Machine Learning*, 1(1–2):1–305, 2008.
- [32] David M Blei, Alp Kucukelbir, and Jon D McAuliffe. Variational inference: A review for statisticians. *Journal of the American statistical Association*, 112(518):859–877, 2017.
- [33] Tamara G. Kolda Brett W. Bader et al. Tensor toolbox for matlab, version 3.4. www.tensortoolbox.org, September 2022.
- [34] Evrim Acar, Daniel M Dunlavy, Tamara G Kolda, and Morten Mørup. Scalable tensor factorizations for incomplete data. *Chemometrics and Intelligent Laboratory Systems*, 106(1):41–56, 2011.
- [35] Lieven De Lathauwer, Bart De Moor, and Joos Vandewalle. On the best rank-1 and rank-(r_1, r_2, \dots, r_m) approximation of higher-order tensors. *SIAM journal on Matrix Analysis and Applications*, 21(4):1324–1342, 2000.
- [36] Shandian Zhe, Kai Zhang, Pengyuan Wang, Kuang-chih Lee, Zenglin Xu, Yuan Qi, and Zoubin Ghahramani. Distributed flexible nonlinear tensor factorization. *Advances in neural information processing systems*, 29, 2016.
- [37] Guangjing Song, Michael K Ng, and Xiongjun Zhang. Robust tensor completion using transformed tensor singular value decomposition. *Numerical Linear Algebra with Applications*, 27(3):e2299, 2020.

A The variational posterior distribution of TT-cores at time t .

$$\begin{aligned}
\log q_{\mathbf{g}_{k,j_d,l}^{(d)}}^{(t)}(\mathbf{g}_{k,j_d,l}^{(d)}) &= \mathbb{E}_{q^{(t)}(\theta \setminus \mathbf{g}_{k,j_d,l}^{(d)})} \left[\log \tilde{p}^{(t)}(\theta) \right] + \text{const} \\
&= \mathbb{E} \left[-\frac{1}{2} \nu_{\mathbf{g}_{k,j_d,l}^{(d)}}^{(t-1)-1} \left(\mathbf{g}_{k,j_d,l}^{(d)} - \mu_{\mathbf{g}_{k,j_d,l}^{(d)}}^{(t-1)} \right)^2 - \frac{\tau}{2} \sum_{\mathbf{j} \in \Omega_t^{j_d}} \left(x_{\mathbf{j}} - \prod_{d=1}^D \mathbf{g}_{j_d}^{(d)} \right)^2 \right] + \text{const} \\
&= \mathbb{E} \left[-\frac{1}{2} \nu_{\mathbf{g}_{k,j_d,l}^{(d)}}^{(t-1)-1} \mathbf{g}_{k,j_d,l}^{(d)2} + \mu_{\mathbf{g}_{k,j_d,l}^{(d)}}^{(t-1)} \nu_{\mathbf{g}_{k,j_d,l}^{(d)}}^{(t-1)-1} \mathbf{g}_{k,j_d,l}^{(d)} - \frac{\tau}{2} \sum_{\mathbf{j} \in \Omega_t^{j_d}} \left(\prod_{d=1}^D \mathbf{g}_{j_d}^{(d)} \right)^2 + \tau \sum_{\mathbf{j} \in \Omega_t^{j_d}} x_{\mathbf{j}} \prod_{d=1}^D \mathbf{g}_{j_d}^{(d)} \right] + \text{const} \\
&= \mathbb{E} \left[-\frac{1}{2} \nu_{\mathbf{g}_{k,j_d,l}^{(d)}}^{(t-1)-1} \mathbf{g}_{k,j_d,l}^{(d)2} + \mu_{\mathbf{g}_{k,j_d,l}^{(d)}}^{(t-1)} \nu_{\mathbf{g}_{k,j_d,l}^{(d)}}^{(t-1)-1} \mathbf{g}_{k,j_d,l}^{(d)} - \frac{\tau}{2} \sum_{\mathbf{j} \in \Omega_t^{j_d}} \prod_{d=1}^D \left(\mathbf{g}_{j_d}^{(d)} \otimes \mathbf{g}_{j_d}^{(d)} \right) + \tau \sum_{\mathbf{j} \in \Omega_t^{j_d}} x_{\mathbf{j}} \prod_{d=1}^D \mathbf{g}_{j_d}^{(d)} \right] + \text{const} \\
&= \mathbb{E} \left[-\frac{1}{2} \nu_{\mathbf{g}_{k,j_d,l}^{(d)}}^{(t-1)-1} \mathbf{g}_{k,j_d,l}^{(d)2} + \mu_{\mathbf{g}_{k,j_d,l}^{(d)}}^{(t-1)} \nu_{\mathbf{g}_{k,j_d,l}^{(d)}}^{(t-1)-1} \mathbf{g}_{k,j_d,l}^{(d)} - \frac{\tau}{2} \sum_{\mathbf{j} \in \Omega_t^{j_d}} b^{(<d)} \left(\mathbf{g}_{j_d}^{(d)} \otimes \mathbf{g}_{j_d}^{(d)} \right) b^{(>d)} + \tau \sum_{\mathbf{j} \in \Omega_t^{j_d}} x_{\mathbf{j}} e^{(<d)} \mathbf{g}_{j_d}^{(d)} e^{(>d)} \right] + \text{const} \\
&= \mathbb{E} \left[-\frac{1}{2} \nu_{\mathbf{g}_{k,j_d,l}^{(d)}}^{(t-1)-1} \mathbf{g}_{k,j_d,l}^{(d)2} + \mu_{\mathbf{g}_{k,j_d,l}^{(d)}}^{(t-1)} \nu_{\mathbf{g}_{k,j_d,l}^{(d)}}^{(t-1)-1} \mathbf{g}_{k,j_d,l}^{(d)} - \frac{\tau}{2} \mathbf{g}_{k,j_d,l}^{(d)2} \sum_{\mathbf{j} \in \Omega_t^{j_d}} b_{(k-1)r_{d-1}+k}^{(<d)} b_{(l-1)r_d+l}^{(>d)} \right. \\
&\quad \left. - \tau \mathbf{g}_{k,j_d,l}^{(d)} \sum_{\mathbf{j} \in \Omega_t^{j_d}} \left(\sum_{k'=1}^{r_{d-1}} \sum_{l'=1}^{r_d} b_{(k-1)r_{d-1}+k'}^{(<d)} b_{(l-1)r_d+l'}^{(>d)} \mathbf{g}_{k',j_d,l'}^{(d)} - b_{(k-1)r_{d-1}+k}^{(<d)} b_{(l-1)r_d+l}^{(>d)} \mathbf{g}_{k,j_d,l}^{(d)} \right) + \tau \mathbf{g}_{k,j_d,l}^{(d)} \sum_{\mathbf{j} \in \Omega_t^{j_d}} x_{\mathbf{j}} e_k^{(<d)} e_l^{(>d)} \right] + \text{const} \\
&= \mathbb{E} \left[-\frac{1}{2} \left(\nu_{\mathbf{g}_{k,j_d,l}^{(d)}}^{(t-1)-1} + \tau \sum_{\mathbf{j} \in \Omega_t^{j_d}} b_{(k-1)r_{d-1}+k}^{(<d)} b_{(l-1)r_d+l}^{(>d)} \right) \mathbf{g}_{k,j_d,l}^{(d)2} + \left(\mu_{\mathbf{g}_{k,j_d,l}^{(d)}}^{(t-1)} \nu_{\mathbf{g}_{k,j_d,l}^{(d)}}^{(t-1)-1} \right. \right. \\
&\quad \left. \left. + \tau \sum_{\mathbf{j} \in \Omega_t^{j_d}} \left(x_{\mathbf{j}} e_k^{(<d)} e_l^{(>d)} - \sum_{k'=1}^{r_{d-1}} \sum_{l'=1}^{r_d} b_{(k-1)r_{d-1}+k'}^{(<d)} b_{(l-1)r_d+l'}^{(>d)} \mathbf{g}_{k',j_d,l'}^{(d)} + b_{(k-1)r_{d-1}+k}^{(<d)} b_{(l-1)r_d+l}^{(>d)} \mathbf{g}_{k,j_d,l}^{(d)} \right) \right) \mathbf{g}_{k,j_d,l}^{(d)} \right] + \text{const} \\
&= -\frac{1}{2} \left(\nu_{\mathbf{g}_{k,j_d,l}^{(d)}}^{(t-1)-1} + \mathbb{E}[\tau] \sum_{\mathbf{j} \in \Omega_t^{j_d}} \mathbb{E} \left[b_{(k-1)r_{d-1}+k}^{(<d)} \right] \mathbb{E} \left[b_{(l-1)r_d+l}^{(>d)} \right] \right) \mathbf{g}_{k,j_d,l}^{(d)2} \\
&\quad + \left(\mu_{\mathbf{g}_{k,j_d,l}^{(d)}}^{(t-1)} \nu_{\mathbf{g}_{k,j_d,l}^{(d)}}^{(t-1)-1} + \mathbb{E}[\tau] \sum_{\mathbf{j} \in \Omega_t^{j_d}} \left(x_{\mathbf{j}} \mathbb{E} \left[e_k^{(<d)} \right] \mathbb{E} \left[e_l^{(>d)} \right] \right. \right. \\
&\quad \left. \left. - \sum_{k'=1}^{r_{d-1}} \sum_{l'=1}^{r_d} \mathbb{E} \left[b_{(k-1)r_{d-1}+k'}^{(<d)} \right] \mathbb{E} \left[b_{(l-1)r_d+l'}^{(>d)} \right] \mu_{\mathbf{g}_{k',j_d,l'}^{(d)}}^{(t-1)} + \mathbb{E} \left[b_{(k-1)r_{d-1}+k}^{(<d)} \right] \mathbb{E} \left[b_{(l-1)r_d+l}^{(>d)} \right] \mu_{\mathbf{g}_{k,j_d,l}^{(d)}}^{(t-1)} \right) \right) \mathbf{g}_{k,j_d,l}^{(d)} + \text{const} \\
\end{aligned} \tag{29}$$

Thus, $q_{\mathbf{g}_{k,j_d,l}^{(d)}}^{(t)}(\mathbf{g}_{k,j_d,l}^{(d)})$ is also a Gaussian distribution

$$q_{\mathbf{g}_{k,j_d,l}^{(d)}}^{(t)}(\mathbf{g}_{k,j_d,l}^{(d)}) = \mathcal{N}(\mathbf{g}_{k,j_d,l}^{(d)} | \mu_{\mathbf{g}_{k,j_d,l}^{(d)}}^{(t)}, \nu_{\mathbf{g}_{k,j_d,l}^{(d)}}^{(t)}), \tag{30}$$

where

$$\begin{aligned}
\nu_{\mathbf{g}_{k,j_d,l}^{(d)}}^{(t)} &= \left(\nu_{\mathbf{g}_{k,j_d,l}^{(d)}}^{(t-1)}^{-1} + \mathbb{E}[\tau] \sum_{\mathbf{j} \in \Omega_t^{j_d}} \mathbb{E} \left[b_{(k-1)r_{d-1}+k}^{(<d)} \right] \mathbb{E} \left[b_{(l-1)r_d+l}^{(>d)} \right] \right)^{-1}, \\
\mu_{\mathbf{g}_{k,j_d,l}^{(d)}}^{(t)} &= \nu_{\mathbf{g}_{k,j_d,l}^{(d)}}^{(t)} \mu_{\mathbf{g}_{k,j_d,l}^{(d)}}^{(t-1)} \nu_{\mathbf{g}_{k,j_d,l}^{(d)}}^{(t-1)}^{-1} + \nu_{\mathbf{g}_{k,j_d,l}^{(d)}}^{(t)} \mathbb{E}[\tau] \sum_{\mathbf{j} \in \Omega_t^{j_d}} \left(x_{\mathbf{j}} \mathbb{E} \left[e_k^{(<d)} \right] \mathbb{E} \left[e_l^{(>d)} \right] \right. \\
&\quad \left. - \sum_{k'=1}^{r_{d-1}} \sum_{l'=1}^{r_d} \mathbb{E} \left[b_{(k-1)r_{d-1}+k'}^{(<d)} \right] \mathbb{E} \left[b_{(l-1)r_d+l'}^{(>d)} \right] \mu_{\mathbf{g}_{k',j_d,l'}}^{(t-1)} + \mathbb{E} \left[b_{(k-1)r_{d-1}+k}^{(<d)} \right] \mathbb{E} \left[b_{(l-1)r_d+l}^{(>d)} \right] \mu_{\mathbf{g}_{k,j_d,l}^{(d)}}^{(t-1)} \right).
\end{aligned} \tag{31}$$

B The variational posterior distribution of the noise precision at time t .

$$\begin{aligned}
\log q_\tau^{(t)}(\tau) &= \mathbb{E}_{q^{(t)}(\theta \setminus \tau)} \left[\log \tilde{p}^{(t)}(\theta) \right] + \text{const} \\
&= \mathbb{E} \left[\left(\alpha^{(t-1)} - 1 \right) \log \tau - \beta^{(t-1)} \tau - \frac{\tau}{2} \sum_{\mathbf{j} \in \Omega_t} \left(x_{\mathbf{j}} - \prod_{d=1}^D \mathbf{g}_{j_d}^{(d)} \right)^2 + \frac{|\Omega_t|}{2} \log \tau \right] + \text{const} \\
&= \mathbb{E} \left[\left(\alpha^{(t-1)} + \frac{|\Omega_t|}{2} - 1 \right) \log \tau - \left(\beta^{(t-1)} + \frac{1}{2} \sum_{\mathbf{j} \in \Omega_t} \left(x_{\mathbf{j}} - \prod_{d=1}^D \mathbf{g}_{j_d}^{(d)} \right)^2 \right) \tau \right] + \text{const} \\
&= \left(\alpha^{(t-1)} + \frac{|\Omega_t|}{2} - 1 \right) \log \tau - \left(\beta^{(t-1)} + \frac{1}{2} \mathbb{E} \left[\sum_{\mathbf{j} \in \Omega_t} \left(x_{\mathbf{j}} - \prod_{d=1}^D \mathbf{g}_{j_d}^{(d)} \right)^2 \right] \right) \tau + \text{const}
\end{aligned} \tag{32}$$

Thus, $q_\tau^{(t)}(\tau)$ is also a Gamma distribution

$$q_\tau^{(t)}(\tau) = \text{Gam}(\tau | \alpha^{(t)}, \beta^{(t)}), \tag{33}$$

and the posterior hyperparameters can be updated by

$$\begin{aligned}
\alpha^{(t)} &= \alpha^{(t-1)} + \frac{|\Omega_t|}{2}, \\
\beta^{(t)} &= \beta^{(t-1)} + \frac{1}{2} \mathbb{E} \left[\sum_{\mathbf{j} \in \Omega_t} \left(x_{\mathbf{j}} - \prod_{d=1}^D \mathbf{g}_{j_d}^{(d)} \right)^2 \right].
\end{aligned} \tag{34}$$

C The log of $\tilde{p}^{(t)}(\theta)$

Since $\tilde{p}^{(t)}(\theta) = q^{(t-1)}(\theta) p(x_{\mathbf{j} \in \Omega_t} | \theta)$, where $\theta = \{\{\mathbf{g}^{(d)}\}_{d=1}^D, \tau\}$, the log of $\tilde{p}^{(t)}(\theta)$ can be written as

$$\begin{aligned}
\log \tilde{p}^{(t)}(\theta) &= \log \left(q^{(t-1)}(\theta) p(B_t | \theta) \right) \\
&= \log q_\tau^{(t-1)}(\tau) + \sum_{d=1}^D \sum_{k=1}^{r_{d-1}} \sum_{l=1}^{r_d} \sum_{j_d=1}^{N_d} \log q_{\mathbf{g}_{k,j_d,l}^{(d)}}^{(t-1)} \left(\mathbf{g}_{k,j_d,l}^{(d)} \right) \log p(x_{\mathbf{j} \in \Omega_t} | \{\mathbf{g}^{(d)}\}_{d=1}^D, \tau) \\
&= (\alpha - 1) \log \tau - \beta \tau - \sum_{d=1}^D \sum_{k=1}^{r_{d-1}} \sum_{l=1}^{r_d} \sum_{j_d=1}^{N_d} \frac{\left(\mathbf{g}_{k,j_d,l}^{(d)} - \mu_{\mathbf{g}_{k,j_d,l}^{(d)}}^{(t-1)} \right)^2}{2 \nu_{\mathbf{g}_{k,j_d,l}^{(d)}}^{(t-1)}} \\
&\quad - \frac{\tau}{2} \sum_{\mathbf{j} \in \Omega_t} \left(x_{\mathbf{j}} - \prod_{d=1}^D \mathbf{g}_{j_d}^{(d)} \right)^2 + \frac{|\Omega_t|}{2} \log \tau.
\end{aligned} \tag{35}$$